Combining 2D and 3D Hand Geometry Features for Biometric Verification

Vivek Kanhangad, Ajay Kumar, David Zhang
Department of Computing, The Hong Kong Polytechnic University, Kowloon, Hong Kong
csvivek@comp.polyu.edu.hk, ajaykr@ieee.org, csdzhang@comp.polyu.edu.hk

Abstract

Traditional hand geometry based personal verification systems offer limited performance and therefore suitable only for small scale applications. This paper investigates a new approach to achieve performance improvement for hand geometry systems by simultaneously acquiring three dimensional features from the presented hands. The proposed system utilizes a laser based 3D digitizer to acquire registered intensity and range images of the presented hands in a completely contact-free manner, without using any hand position restricting mechanism. Two new representations that characterize the local features on the finger surface are extracted from the acquired range images and are matched using the proposed matching metrics. The proposed approach is evaluated on a database of 177 users, with 10 hand images for each user acquired in two sessions. Our experimental results suggest that the proposed 3D hand geometry features have significant discriminatory information to reliably authenticate individuals. Our experimental results also demonstrate that the combination of 3D hand geometry features with 2D geometry features can be employed to significantly improve the performance from 2D hand geometry features alone.

1. Introduction

Hand geometry based biometric systems exploit features on the human hand to perform identity verification. Due to limited discriminatory power of the hand geometry features, these systems are rarely employed for applications that require performing identity recognition from a large scale database. Nevertheless, these systems have gained immense popularity and public acceptance as evident from their extensive deployment for applications in access control, attendance tracking and several other verification tasks.

A number of techniques for personal verification based on hand geometry features have been proposed in the literature [1]-[3]. Often, users are required to place their hand on flat surface fitted with pegs to minimize variations in the hand position. Though use of such constraints make the feature extraction task easier and consequently result in lower error rates, such systems are not user friendly. For example, elderly or people with arthritis and other conditions that limit dexterity may have difficulty placing their hand on a surface guided by pegs. In order to overcome this problem, a few researchers have proposed to do away with hand position restricting pegs [4], [9], [10], [13], [17]. Feature extraction algorithm in their approaches takes care of possible rotation or translation of the hand images acquired without guiding pegs. However with the notable exception in [17], users are still required to place their hand on a flat surface or a digital scanner. Such contact raises security as well as hygienic concerns among users. Moreover, most of the hand geometry systems/techniques proposed in the literature are based on users' gray level hand images. These approaches extract various features from the binarized version of the acquired hand image. Unique information in such binary images is very limited, leading to low discriminatory power from the hand geometry biometric systems. With the advent of advanced 3D data acquisition devices, researchers have investigated the use of 3D features for face [15] and ear [16] biometrics. A few researchers have also explored 3D hand/finger information for identity verification and recognition [5]-[6]. The objective of this work is to further explore 3D hand/finger geometry features and to build a robust and reliable hand geometry system, without sacrificing user friendliness and acceptability. The contributions of this paper can be summarized as follows. Firstly, two new representations that explicitly capture the finger surface details are proposed. Secondly, we investigate how much performance improvement can be achieved by combining 2D and the proposed 3D hand geometry information. Finally, the proposed system is evaluated on a large database of intensity and range hand images to ascertain more reliable estimate of the performance.

2. System description

The block diagram of the proposed biometric system that can simultaneously employ 2D and 3D hand geometry features is shown in Figure 1. Major computational modules of the proposed system are in image normalization (in the pre processing stage), feature extraction and feature matching stages. The details of these key processing stages appear in the following sections.

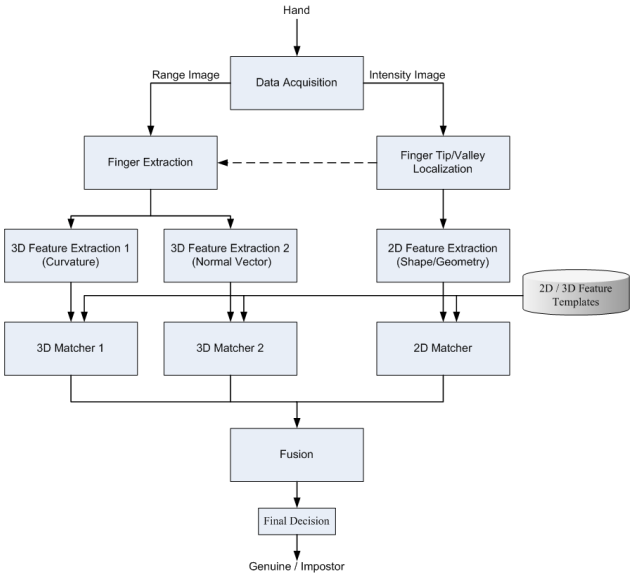

Figure 1. Block diagram of the proposed system

2.1. Pre processing and finger extraction

The acquired intensity images are first processed to automatically locate the finger tips and finger valleys. These reference points are then used to determine the orientation of each finger and to extract them from the input hand image. Since there is a pixel-to-pixel correspondence between the acquired intensity and range image, we work only on the intensity image to determine key points and orientation. The steps involved in the process of locating and extracting fingers are illustrated in Figure 2. To start with, the acquired intensity image is binarized using Otsu's threshold [7]. Resulting binary image is further processed using morphological opening to remove small pixel regions that are not part of the hand. Boundary pixels of the hand in the processed binary image are then identified using the 8-connected contour tracing algorithm [18]. Traversing the extracted hand contour, local minima and local maxima which correspond to finger tips and finger valleys, can easily be located. In order to estimate the orientation of each finger, four points on the finger contour (two points each on both sides of the fingertip) at fixed distances from the finger tip are identified. Two middle points are computed for corresponding points on both side and are joined to obtain the finger orientation. This approach is similar to the one employed in [10] to automatically find the line of symmetry.

However, differing from their approach, we only consider points on the finger contour that are close to the finger tip. Points at the center and bottom part of the finger are not considered for estimation of orientation, as some of the fingers were found to be non-symmetric at these parts. Having determined the finger orientation and finger tip/valley points, it is straightforward task to extract a rectangular region of interest for fingers. Figure 2(e) shows the extracted region of interests for four fingers. The process of finger extraction discussed above can handle rotation and translation of the hand in the image plane, which are inevitable in a peg free data acquisition set up.

2.2. 3D finger modeling and feature extraction

Based on the finger localization algorithm discussed in the previous section, individual fingers can be located and extracted from the acquired hand range image. Figure 3(a) shows the 3D visualization for a finger extracted from range image of the hand. Each of the four finger range images is further processed for feature extraction. 3D Feature extraction technique adopted in this work is motivated by the conventional finger width features employed in the hand geometry verification. For each of the finger, a number of cross sectional segments are extracted at uniformly spaced distances along the finger length (see figure 3(b)).

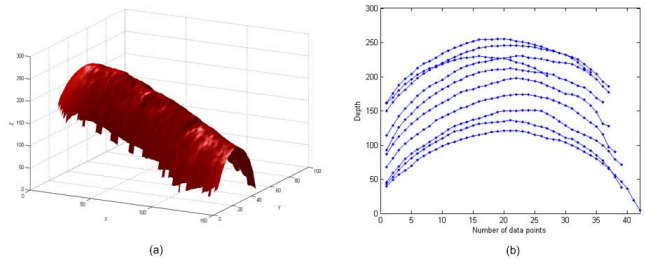

Figure 3. (a) Rendered view of a 3D finger surface and (b) extracted cross sectional segments

The next step in the feature extraction process is to compute two representations, namely, mean curvature and unit normal vector, for every data point on the extracted segments. In order to compute these features, we first use a two dimensional polynomial to model the data point and its neighbors. The mean curvature and normal vector features can then be computed for the fitted 2D polynomial by estimating numerical partial derivates of the polynomial at

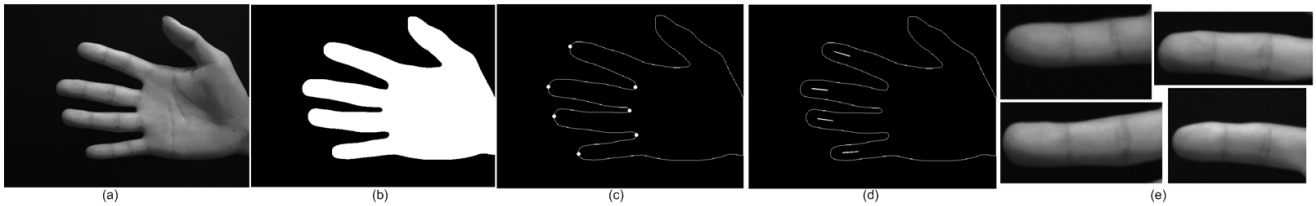

Figure 2. Pre-processing and finger extraction: (a) Input intensity image, (b) Binary hand image after thresholding and morphological operations, (c) Finger tips and valleys located, (d) Detected finger orientations, (e) Extracted individual fingers

each data point. Savitzky-Golay filters [11] are widely used to fit one dimensional polynomial and compute its numerical derivatives. The concept of one dimensional Savitzky-Golay filters can be easily extended to two dimensional polynomial fitting. In our experiments, we used the MATLAB code for two dimensional Savitzky-Golay filters available at [12]. The 2D polynomial $f(x, y)$ employed in this work has the following form

$$f(x,y) = c_{00} + c_{10}x + c_{01}y + c_{11}xy + c_{20}x^2 + c_{02}y^2 \quad (1)$$

where x and y are the two dimensional coordinates of a data point. The degree of the polynomial (=2) in the above equation and the neighborhood size N (5 × 5) are determined empirically. In order to model the data point and its neighbors represented by a vector $\mathrm{d} = [d(0)\ d(1)\ \ldots\ d(N)]^{\mathrm{T}}$, a matrix equation can be formulated as

$$\mathrm{M} \times \mathrm{c} = \mathrm{d} \quad (2)$$

where each of N rows of the matrix M takes the value $[1\ x_i\ y_i\ x_i y_i\ x_i^2\ y_i^2]$ with $i = 0,1,\ldots,N-1$ and c is the column vector of polynomial coefficients. The above equation can easily be solved for polynomial coefficients by least squares approach. The next step in our approach is to extract features from the fitted polynomial. The expression for mean curvature of a 2D polynomial in terms of its coefficients is given by

$$\kappa_{2D} = \frac{(1+c_{10}^2)c_{02} + (1+c_{01}^2)c_{20} - c_{10}c_{01}c_{11}}{(1+c_{10}^2+c_{01}^2)^{3/2}} \quad (3)$$

Mean curvature in equation 3 is computed for every data point on the cross sectional segments and stored as feature templates in the database. Figure 4(a) shows a cross sectional finger segment extracted from the 3D finger and the corresponding mean curvature plot (in figure 4(b)). Note the presence of detail information (of finger surface) in this curvature plot. It is clear from these figures that the feature extraction approach employed in this work effectively captures the local curvature information on the finger surface.

In addition to the curvature feature, we also compute surface normal vector at every data point on the segment. Assume a parametric surface is defined as

$$\mathrm{p}(x,y) = (x, y, z(x,y)) \quad (4)$$

Since the surface normal is parallel to the cross product of partial derivatives of this surface with respect to x and y, it can be obtained as follows:

$$\mathrm{n} = \frac{\partial \mathrm{p}}{\partial x} \times \frac{\partial \mathrm{p}}{\partial y} \quad (5)$$

Computing the above cross product, expression for unit normal vector at each data point (in terms of the fitted polynomial coefficients) can be further simplified as follows:

$$\mathrm{n}_u = \frac{1}{\sqrt{1+c_{10}^2+c_{01}^2}}(-c_{10}, -c_{01}, 1) \quad (6)$$

Figure 5 shows the normal vector features extracted for an extracted finger segment. These computed normal vectors are also stored as feature templates for matching in the following stage.

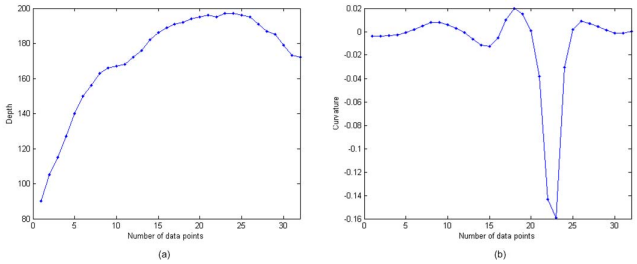

Figure 4. (a) A cross sectional finger segment and (b) its computed curvature features

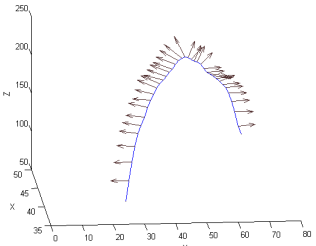

Figure 5. Normal features computed for a finger segment

2.3. 3D feature matching

In order to match 3D finger features, two simple and efficient matching metrics are introduced. The proposed metrics can effectively handle small changes in hand pose, i.e., deviation of the hand position from being parallel to the image plane of the scanner. Features extracted from each of the four fingers are matched individually and then combined to obtain a final matching score.

Assume we have extracted features for N_s number of cross sectional segments from template and probe (query) fingers represented by T_i and Q_i respectively, where the subscript i represents the index for fingers and takes values from 1 to 4 for little, ring, middle and index fingers. Matching of curvature features from a corresponding pair of fingers (denoted as s_i^c) is based on the cosine similarity metric and the match score is computed as

$$s_i^c = \frac{1}{N_s}\sum_{j=1}^{N_s}\phi_i^j, \quad \text{where} \quad \phi_i^j = \begin{cases} \dfrac{T_i^j . Q_i^j(1:l_T^j)}{\left|T_i^j\right|\left|Q_i^j(1:l_T^j)\right|} & \text{if} \quad l_T^j < l_Q^j \\ \dfrac{T_i^j(1:l_Q^j) . Q_i^j}{\left|T_i^j(1:l_Q^j)\right|\left|Q_i^j\right|} & \text{otherwise} \end{cases} \quad (7)$$

where l_T^j and l_Q^j are the number of feature points on the j^{th} cross sectional segment of the template (T_i^j) and query (Q_i^j)fingers respectively. The number of feature

points l_T^j and l_Q^j cannot be guaranteed to be equal, even when they are from corresponding fingers (from different samples) of the same user. This is because, the feature points are computed at every data point on the cross sectional segment and the number of these data points recorded by the scanner varies from one sample to another. Therefore we perform multiple matches by sliding the shorter feature vector over the longer one and taking the best score among them as the final match score. By this approach, we are also able to handle slight changes in hand pose.

Matching of unit normal vector features is performed in a manner similar to the one described for curvature features. Angle in radians between two feature points is considered to be the degree of agreement (match) between them. For a template and query finger represented by T_i and Q_i, the match score is computed as

$$s_i^n = \frac{1}{N_s}\sum_{j=1}^{N_s}\phi_i^j, \quad \text{where} \quad \phi_i^j = \begin{cases} \cos^{-1}(T_i^j . Q_i^j(1:l_1)) & if \quad l_T^j < l_Q^j \\ \cos^{-1}(T_i^j(1:l_2) . Q_i^j) & otherwise \end{cases} \quad (8)$$

Match scores generated for four fingers by individually matching corresponding fingers are then averaged to obtain the final score for 3D normal feature. Finally, the simple weighted sum rule is applied to combine scores from the two matchers. Therefore, 3D finger match score $S_{3DFinger}$ is given by

$$S_{3DFinger} = w_1 \times S_{curv} + (1 - w_1) \times S_{norm} \quad (9)$$

where S_{curv} $(= \frac{1}{4}\sum_{i=1}^{4} s_i^c)$,and S_{norm} $(= \frac{1}{4}\sum_{i=1}^{4} s_i^n)$ are the final scores generated from curvature and normal feature matching as illustrated above. w_1 is the empirically determined weight parameter for combining 3D finger representations.

3. Experiments and Results

Performance of the proposed multimodal system is evaluated on a database of 3,540 right hand images collected from 177 persons. Since there is no publicly available database of 3D and 2D hand images (with the palm side scanned), we set up one at our university. The details of our data collection process are described in the following section.

3.1. 3D hand image database

A 3D hand image database was acquired using a Minolta Vivid 910 range scanner [8]. 177 persons participated in the data collection process that spanned over 4 months. Participants were mainly students and staff at our university and were in the age group of 18 to 50 years, with multiple ethnic backgrounds. Each person contributed 5 hand images (range and a registered intensity image acquired simultaneously) in the first session, followed by another 5 in the second session. Therefore our database currently has 3,540 hand images (of 3D and corresponding 2D). The time interval between two data collection sessions was not uniform for all the persons; instead it ranged from one week to three months. All images were acquired in the indoor environment, with no restrictions on the illumination. In fact, our data collection process was carried out at three different locations which had notable variations in surrounding illumination. During the image acquisition, every user is expected to holds his/her right hand in front of the scanner at a distance of about 0.7 m, chosen to maximize the relative size of the hand in the acquired images. No constraints were employed to confine the position of the hand nor were the users required to remove any hand jewelry that in case they were wearing. However, in order to simplify the hand segmentation task, the background behind the user's hand was ensured to be of black color.

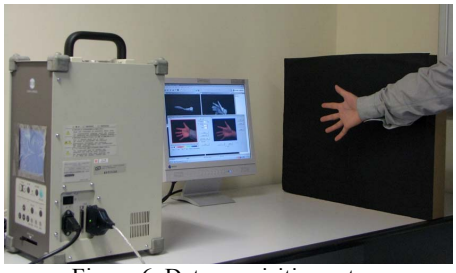

Figure 6. Data acquisition set up

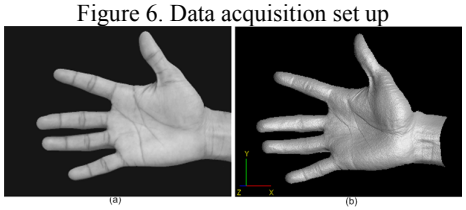

Figure 7. An example of the data captured. (a) Intensity image and (b) rendered view of 3D hand

Users were only requested to hold their hand with their palm approximately parallel to the image plane of the scanner and inside the imaging area. This task was facilitated by providing the users a live visual feedback of positioning of the hand. In order to introduce variations in the database, users were asked to change their hand position after each image acquisition. Figure 6 shows a picture of the data acquisition set up employed in this work. Sample of representative hand images (range as well as intensity) from the acquired database are shown in Figure 7.

3.2. Results

Two sets of experiments are carried out in verification mode to obtain a performance estimate of the proposed system. In the first set, we evaluate the individual performance of the proposed 3D hand geometry features,

while in the second, improvement in performance that can be achieved by combining 3D and 2D hand geometry features is investigated. For each user, five image samples collected in the first session are used to generate feature templates. Five hand images collected in the second session constitute the query samples. A set of genuine scores are generated by matching features from each of the query samples with the user's feature templates and taking the best score among them as the final match score. The same approach is followed for generating impostor scores. False Acceptance Rate (FAR) and False Reject Rate (FRR) are then computed and are used to plot the Receiver Operating Characteristics (ROC) curve. Figure 9 shows the ROC curves for the proposed 3D hand geometry features. It also depicts the overall 3D hand geometry performance resulting from the combination of curvature and normal features. These features are combined using weighted sum rule as in equation 9, with empirically selected weights 0.7 and 0.3 for curvature and normal features respectively. Empirical selection of weights was based on the performance on an independent training set, with genuine and impostor scores generated using the five samples collected in the first session. As shown in figure 9, the combination of the proposed 3D hand geometry features achieves an Equal Error Rate (EER) of 3.8%. This result clearly demonstrates that features extracted from 3D hand images carry significant discriminatory information to authenticate individuals. Moreover, the proposed 3D hand geometry features can be efficiently combined with simultaneously extracted 2D features to further improve the performance of the system.

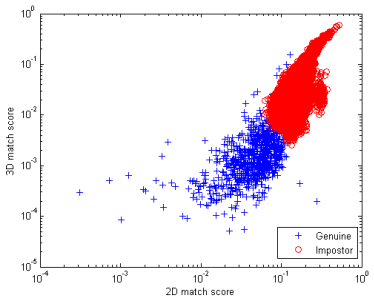

Figure 8. Distribution of genuine and impostor scores

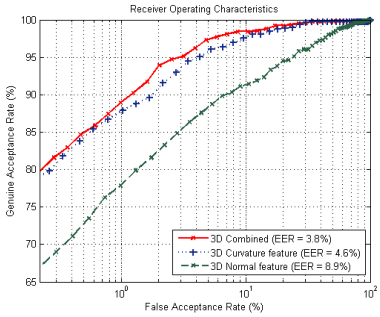

Figure 9. ROC curves for individual 3D hand geometry representations and the combined performance

Second set of experiments are performed to obtain an estimate for the performance gain resulting from combination of the 3D and 2D hand geometry features. The 2D hand geometry features considered in this study are – finger length, finger widths at equally spaced distances along the finger length, finger area and perimeter. Matching of template and query feature vectors is based on the simple Euclidean distance. Genuine and impostor match score distributions for 2D and 3D matchers are shown in figure 8. Again, scores corresponding to 3D and 2D hand geometry features are combined using a weighted sum rule. Results from our second experiment are summarized in figure 10, with ROC curves for 2D, 3D as well as their combination. Table 1 summarizes the EER achieved from the corresponding features employed in our experiments.

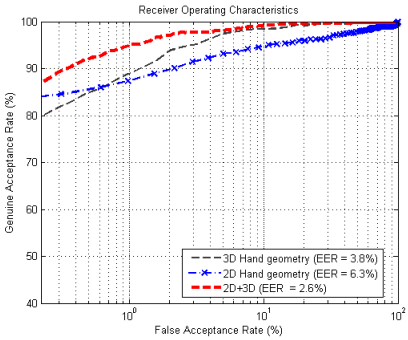

Figure 10. ROC curves for the proposed 3D hand geometry representations, 2D features and their combination.

As shown in figure 10, combining simultaneously extracted 2D hand geometry features along with the proposed 3D features helps improve the overall system performance (EER) by about 30 percent. Table 2 provides a summary of performances from related works in the literature and the one proposed in this paper. One can observe that the performance from the proposed approach (on a relatively larger database) is quite comparable, or better, with other approaches reported in the literature. However, one should also note that a one-to-one comparison of the approaches cannot be made as these performance statistics are obtained on different datasets, with non-standard experimental configurations.

Table 1: Performance indices from the experiments

Hand Geometry Matcher	EER (%)
3D	3.8
2D	6.3
(2D+3D)	2.6

4. Conclusions

This paper has presented a new approach to achieve more reliable personal authentication using simultaneous extraction and combination of 3D and 2D hand geometry features. The proposed system acquires hand images in a

Table 2: Summary of related work on hand geometry based authentication

Authors	Methodology	No. of Templates	Performance	Database size (Users)
Jain and Duta [3]	Individual finger shapes are aligned and a *shape distance* is computed as match score	1-14	FAR – 2% FRR – 3.5%	53
Jain et al. [2]	Measurements are made along 16 different axes, matched using weighted Euclidean distance	1(Averaged)	FAR – 2% FRR – 15%	50
Sanchez-Reillo et al. [1]	Feature vector comprises several width, height and angle measurements. GMM is used for matching	1(Averaged)	FAR – 6% FRR – 6%	20
Woodard and Flynn [6]	Shape index image is extracted from range images of fingers and is matched using normalized correlation coefficient	1(Averaged)	FAR – 5.5% FRR – 5.5%	177(probe) 132(gallery)
Malassiotis et al. [5]	96 curvature and 3D finger width measurements matched using L_1 distance	4	FAR – 3.6% FRR– 3.6%	73
Xiong et al. [9]	Aligns individual finger shapes using a elliptical model and finger tip/valley information	1	FAR – 2.4% FRR – 2.4%	108
Kumar et al. [4]	16 geometry measurements matched using normalized correlation	5	FAR – 5.3% FRR – 8.2%	100
Lay [14]	Coding of distorted pattern of the back of hand by quad tree	Not available	FAR – 0% FRR – 3.9%	100
This Paper	Fusion of the proposed 3D and 2D hand geometry features	5	FAR – 2.6% FRR – 2.6%	177

contact-free manner to ensure high user friendliness and also to address the hygienic concerns. Simultaneously acquired range and 2D images of the hand are processed for the feature extraction and matching. We introduced two new representations, namely, finger surface curvature and unit normal vector, for 3D hand geometry based biometric measurement. Simple and efficient metrics are proposed for the matching of pair of 3D hand images. Match scores from 3D and 2D hand geometry matchers are combined to obtain a highly reliable authentication system. Our experimental results on a database of 177 subjects demonstrate that the 3D hand geometry features have high discriminatory information for biometric verification. Our experimental results also demonstrate that the significant performance improvement can be achieved by combining hand geometry information extracted from user's 2D and 3D hand images.

References

[1] R. Sanchez-Reillo, C. Sanchez-Avila, and A. Gonzalez-Macros, "Biometric Identification through Hand Geometry Measurements", IEEE Trans. PAMI, 22(10):1168-1171, Oct. 2000.

[2] A. K. Jain, A. Ross, and S. Pankanti, "A Prototype hand geometry-based verification system", Proc. AVBPA, Washington DC,166-171, Mar.1999.

[3] A. K. Jain, and N. Duta, "Deformable matching of hand shapes for verification", Proc. International Conf. Image Processing, 857-861, Oct.1999.

[4] A. Kumar, D. C. M. Wong, H. C. Shen, and A. K. Jain, "Personal verification using palmprint and hand geometry biometric", Proc. AVBPA, Guildford, U.K., 668-675, 2003.

[5] S. Malassiotis, N. Aifanti, and M. G. Strintzis, "Personal Authentication using 3-D finger geometry", IEEE Trans. Info. Forensics & Security, 1(1): 12-21, Mar. 2006.

[6] D. L. Woodard and P. J. Flynn, "Finger surface as a biometric identifier", CVIU, 100(3): 357-384, Dec. 2005.

[7] N. Otsu, "A threshold selection method from gray-level histograms", IEEE Trans. Systems, Man and Cybernetics, 9(1):62–66, 1979.

[8] Minolta Vivid 910 noncontact 3D digitizer, http://www.konicaminolta.com/instruments/products/3d/non-contact/vivid910/index.html, 2008.

[9] W. Xiong, K.A. Toh, W.Y. Yau, X. Jiang, "Model-guided deformable hand shape recognition without positioning aids", Pattern Recognition, 38(10): 1651-1664, Oct. 2005.

[10] S. Ribaric, and I. Fratric, "A Biometric Identification System Based on Eigenpalm and Eigenfinger Features", IEEE Trans. PAMI, 27(11), Nov. 2005.

[11] W.H. Press, S. A. Teukolsky, W.T. Vetterling, B.P. Flannery, Numerical recipes: the art of scientific computing, Cambridge University Press, 2007.

[12] Savitzky-Golay filters for 2D images, http://research.microsoft.com/enus/um/people/jckrumm/savgol/savgol.htm, 2008.

[13] A. Kumar and Ch. Ravikanth, "Personal authentication using finger knuckle surface", IEEE Trans. Info. Forensics & Security, 4(1): 98-110, Mar. 2009.

[14] Y.L. Lay, "Hand shape recognition", Opt. Laser Technol. 32 (1): 1–5, 2000.

[15] K. I. Chang, K. W. Bowyer, and P. J. Flynn, "An evaluation of multimodal 2D+3D face biometrics", IEEE Trans. Pattern Anal. Mach. Intell., 27(4): 619-624, Apr. 2005.

[16] H. Chen, B. Bhanu, "Human ear recognition in 3D", IEEE Trans. Pattern Anal. Mach. Intell., 29(4): 718-737, Apr. 2007.

[17] A. Kumar, "Incorporating cohort information for reliable palmprint authentication," Proc. ICVGIP, 583-590, Dec. 2008.

[18] M. Sonka and R. Hlavac, V. Boyle, *Image Processing, Analysis, and Machine Vision*, PWS Publishing, 1999.